Adsorbate-Induced Expansion of Silicalite-1 Crystals

Stephanie G. Sorenson,[†] Joseph R. Smyth,[‡] Milan Kocirik,[§] Arlette Zikanova,[§] Richard D. Noble,[†] and John L. Falconer*,[†]

Department of Chemical and Biological Engineering and Department of Geological Sciences, University of Colorado, Boulder, Colorado 80309, and J. Heyrovsky Institute of Physical Chemistry, Academy of Sciences of the Czech Republic, Dolejskova 3, 182 23 Praha 8, Czech Republic

Optical microscopy and XRD measurements show that silicalite-1 crystals expand when C_4-C_8 alkanes and *i*-butane adsorb in the MFI structure at room temperature. The *c*-direction linear expansion was 0.20−0.45%, and was measured with XRD and optical microscopy for 200 μm crystals. *n*-Pentane, *n*-hexane, and *n*-heptane had the maximum linear expansion of approximately 0.54% in the *b*-direction, and *n*-hexane and *n*-heptane had the maximum volume expansion of 1.2%. In contrast, benzene did not cause a significant change in the unit cell volume. The *a*-direction expanded least for the molecules studied except *i*-butane. *n*-Hexane expanded the silicalite-1 crystal more at 180 K than at room temperature. Crystal expansion due to *n*-alkane adsorption decreased the size of defects in a polycrystalline MFI membrane, and changes in the fluxes of *i*-octane through defects were measured by transient permeation. Loadings as low as 0.5 molecule/unit cell decreased the flux through defects at 358−473 K, but benzene had no effect. Higher loadings increased crystal expansion and decreased the defect size more. Crystal expansion was reversible.

Introduction

Zeolite membranes have uniform pore sizes, chemical and thermal stability, and the ability to perform difficult separations. Because MFI zeolite membranes have pores that are similar in size to small organic molecules, they have been studied more than other types of structures. The MFI structure has straight and sinusoidal channels with dimensions of 0.53 nm × 0.56 nm and 0.51 nm × 0.55 nm respectively, as determined by XRD.[1] However, the pores are large enough to absorb molecules with kinetic diameters of at least 0.6 nm.[2] Polycrystalline MFI membranes, such as silicalite-1 and the analogous BZSM-5,[3] can separate hydrocarbon isomers, such as *n*-hexane and 2,2-dimethylbutane (DMB), but defects (grain boundaries or non-zeolitic pores) between the crystals limit selectivity.

Studies reported *n*-hexane/DMB separations selectivities greater than 500[4−9] that were attributed to preferential adsorption of *n*-hexane[6−8] and size exclusion.[6,7,9] Recent studies, however, indicated that adsorption of *n*-hexane and *n*-octane decreased the defect sizes in MFI membranes,[10−13] and thus their separation selectivity was higher than their ideal selectivity. The decrease was attributed to MFI crystal expansion, so a membrane that initially had significant flow through defects could separate difficult-to-separate mixtures such as organic isomers.

Yu et al. found that low concentrations of *n*-hexane in a liquid mixture with DMB shrank the defect pores sufficiently to decrease the DMB flux by almost 2 orders of magnitude during pervaporation.[10] The DMB only diffused through defects at the conditions used. Thus, the *n*-hexane/DMB separation selectivity during pervaporation was 900 times the ideal selectivity.[10] Similarly, for a membrane in which most of the benzene flux was through defects, the benzene flux decreased to 2% of its single-component value when 1.4% *n*-hexane was added to benzene.[11]

Temperature-programmed desorption showed that adsorption decreased the nonzeolite pore volume in a MFI membrane.[12] When *n*-hexane adsorbed in the MFI structure, the amount of DMB adsorbed in the defects was less than half the amount adsorbed in the absence of *n*-hexane. A decrease was seen for loadings greater than three *n*-hexane or *n*-octane molecules per unit cell (molec/u.c.). In contrast, benzene had little effect on the defect volume. Permporosimetry measurements demonstrated that *n*-pentane, *n*-butane, propane, and SF_6 also decreased the flux through defects in MFI membranes.[12] These changes in pore volume and fluxes were attributed to MFI crystal expansion, but direct measurements of crystal expansion were not made.

Studies using XRD have shown that zeolite crystals deform due to changes in pressure,[14] temperature,[15−20] and adsorption.[2,21−32] The volume of silicalite-1 and ZSM-5 crystals decreased as the temperature increased;[15−18] the percent volume decrease ranged from 0.47% (from 300 to 1040 K)[17] to 2.2% (from room temperature to 567 K).[16] Water adsorption at room temperature shrank the MFI unit cell volume by 0.25%,[19] whereas benzene expanded MFI crystals by 0.26 vol % at room temperature.[29] *n*-Hexane expanded MFI crystals by 2.2 vol % at 180 K.[28,30] Boulicaut et al. proposed, based on adsorption and diffusion studies, that high loadings of *n*-hexane expanded the unit cell of silicalite-1.[33] Mentzen et al. reported that unit cell dimensions depended on p-xylene loading. At 2 molec./u.c. the volume decreased by 0.02%, while at 4 and 8 p-xylene molec/u.c. the volume expanded 0.03 and 0.39%, respectively.[25]

In the current study, XRD and optical microscopy were used to measure the changes in size and unit cell parameters of large silicalite-1 crystals for benzene, *i*-butane, and C_4 to C_8 alkane adsorption at room temperature. These measurements demonstrate that adsorption could cause defect sizes to decrease in MFI membranes by expanding silicalite-1 crystals. Optical microscopy could be used as a quick screening method, but it only had sensitivity to measure changes for crystal dimensions of approximately 200 μm or larger. The changes in crystal sizes were compared to transient measurements of fluxes of a large molecule through defects in MFI membranes at room temper-

* To whom correspondence should be addressed. E-mail: john.falconer@colorado.edu. Tel.: (303) 492-8005.
[†] Department of Chemical and Biological Engineering, University of Colorado.
[‡] Department of Geological Sciences, University of Colorado.
[§] Academy of Sciences of the Czech Republic.

10.1021/ie800630g CCC: $40.75
Published on Web 10/29/2008

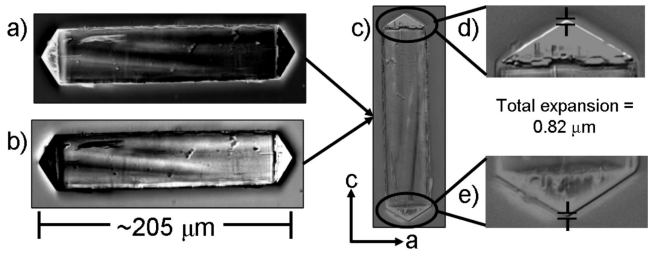

Figure 1. Inverted microscope images: (a) negative image of a MFI crystal before adsorption, (b) positive image after n-C_6 adsorption; (c) superimposed images; (d, e) enlargements showing crystal growth (white area in panel d and black area in panel e).

ature. Transient measurements could be more readily carried out at high temperatures than XRD or optical microscopy. Measurements were made at 473 K, which is higher than temperatures used previously to show that fluxes through defects decreased, and these measurements were more easily made for low loading of adsorbates than XRD or optical microscopy measurements.

Experimental Methods

Silicalite-1 Crystals. Large silicalite-1 crystals were synthesized by the method of Kornatowski[34] with crystal dimensions of L_a (length of a-direction) $\approx L_b \approx 45$ μm and $L_c \approx 200$ μm.[35,36] References 35 and 36 describe the properties of large silicalite-1 crystals and reveal the grain boundaries in twinned silicalite-1 crystals and polycrystalline layers. Selected-area electron diffraction patterns showed that the crystals were twinned on the 110 plane, resulting in the four lateral faces being 100.[37] Figure 1 shows the crystal unit cell directions. X-ray powder diffraction showed the uncalcined silicalite-1 to be orthorhombic, with the *Pnma* space group and the unit cell of $a = 2.00801(2)$ nm, $b = 1.99239(2)$ nm, and $c = 1.34167(1)$ nm.[37]

X-ray Diffraction. Individual crystals were wedged into glass capillaries to secure them for XRD measurements. The glass capillary was ~1.3 mm in diameter and necked down to 80 μm. This allowed liquid to remain in the capillary during XRD analysis without touching the crystal. The crystals were calcined at 723 K for 6 h with a heating rate of 36 K/h and a cooling rate of 54 K/h. Immediately after cooling, an excess of the molecule of interest was added to the capillary so that liquid remained in the capillary after the crystal was saturated. One end of the capillary was sealed with wax, while the tapered end remained open to the atmosphere. The capillary was placed on a goniometer and the orientation matrix was determined using a Bruker APEX II charge coupled device detector on a Bruker P4 diffractometer on a Mo rotating-anode X-ray source operated at 50 kv and 250 mA and an exposure time of 10 s per image.

The goniometer was then transferred to a Bruker P4 diffractometer with a point detector for high-precision, cell parameter measurement. The orientation matrix determined from the CCD was used for initial orientation. For each crystal approximately 18 to 24 reflections were centered in both positive and negative two-θ. The four diffractometer angles were refined for each reflection and the unit cell parameters refined from the centered angles. The three crystals used for XRD analysis were calcined between runs.

Optical Microscopy. Single crystals were placed on glass microscope slides and calcined at 723 K for 8 h. The slide was placed on a Nikon inverted optical microscope, and the image focused using a 40× lens. After an image was taken at room temperature, drops of a hydrocarbon were placed on the slide near the crystal without touching or moving the crystal. Another crystal image was taken after exposure. The exposure time depended on the chemical used.

Crystal lengths were measured by stretching the image from black to white so that the darkest area of the image was set to black and the lightest area was set to white. This resulted in a light edge and dark edge due to lighting and microscope focus. The image was then zoomed to 1600×, and the crystal length measured from the darkest pixel of the crystal to the lightest with a detection limit of 0.01 μm. Figure 1 shows a negative image of a crystal before adsorption (Figure 1a) and a positive image of a crystal after n-hexane adsorption (Figure 1b). The two images were superimposed (Figure 1c), and an enlarged view of the edge is shown in Figure 1d,e. The thin, black (1d) and white areas (1e) had a total width of approximately 0.8 μm due to crystal expansion. No optical distortion due to chemicals was found when tested with gold foil. Because of the microscope resolution, only changes in the c-direction, the largest dimension of the crystal, could be measured.

MFI Membrane. The MFI membrane was synthesized by in situ crystallization onto the inside of a tubular α-alumina support (0.2-μm pores, Pall Corp.). Two ends of the support were sealed with a glazing compound (IN1001, Duncan). The glaze was fired at 1170 K for 30 min with heating and cooling rates of 1.2 K/min. The permeate area was approximately 5.1 cm^2. Before synthesis, the support was boiled in deionized (DI) water twice, each for 30 min, and dried at 373 K under vacuum for 30 min. The synthesis gel had a molar composition of 4.44 TPAOH:19.5 SiO_2:1.55 $B(OH)_3$:500 H_2O.[38] One end of the support tube was wrapped with Teflon tape and plugged with a Teflon cap, and the inside of the support was filled with ~2 mL of synthesis gel. The other end was then plugged with a Teflon cap and left overnight at room temperature. The porous support soaked up almost all the synthesis gel. The tube was again filled with gel, plugged with a Teflon cap, and put into an autoclave at 458 K for 24 h. The membrane was then brushed to remove loose crystals, washed with DI water, and dried. A second and third synthesis was carried out using the same procedure, but the tube was not soaked with the gel overnight, and the membrane's vertical orientation in the autoclave was switched. The resulting membrane was calcined at 700 K for 8 h with heating and cooling rates of 0.6 and 0.9 K/min.

Permporosimetry. Permporosimetry was used to determine the fraction of helium flow through defects.[11,12] A hydrocarbon (benzene or n-hexane) was added to a helium stream that flowed through two liquid bubblers in series at 292 K, and this stream was mixed with a second helium stream. The flow rates of the helium streams were changed with mass flow controllers to obtain desired hydrocarbon activities. The pressure difference across the membrane was 96 kPa, and the permeate pressure was 84 kPa. The permeate flux of helium was measured with a bubble flow meter and a mass flow meter as a function of hydrocarbon activity. An activated carbon trap removed the hydrocarbon from the permeate stream so that only helium flow was measured. The hydrocarbon adsorbed in the MFI structure and blocked helium flow through those pores at high loadings so that the remaining helium flow was through defects.

Transient Permeation. Transient permeation was carried out in a Wicke−Kallenbach system.[39] Mass flow controllers controlled the feed and sweep flow rates, which were 100 cm^3 (STP) min^{-1}. All hydrocarbons were ≥99.0% pure and ultra high purity helium (>99.99%) was used. Syringe pumps were used

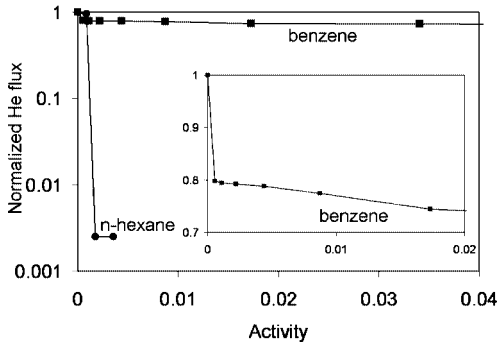

Figure 2. Logarithmic plot of helium flux at room temperature as a function of benzene and *n*-hexane activity during permporosimetry. The insert is linear plot of helium flux as a function of benzene activity.

Table 1. Uncalcined MFI Zeolite Unit Cell Parameters from XRD Measurements at Room Temperature

	other studies				current study
	powder[37]	powder[47]	single crystal[47]	single crystal[46]	single crystal
a (nm)	2.00801 (2)	2.0117 (5)	2.0044 (2)	2.007 (1)	2.0058 (1)
b (nm)	1.99239 (2)	1.9874 (5)	1.9918 (4)	1.992 (1)	1.9924 (1)
c (nm)	1.34167 (1)	1.3371 (4)	1.3395 (2)	1.342 (1)	1.3383 (1)
vol (nm^3)	5.3678 (4)	5.346 (2)	5.348 (1)	5.365 (6)	5.3483 (6)

to feed the hydrocarbon liquids. The *n*-hexane, *n*-octane, and benzene loadings were calculated using literature isotherms.[40−42]

Initially, an *i*-octane/helium stream (feed A) flowed through the membrane and a hydrocarbon/*i*-octane/helium stream (feed B) flowed to the vent. Feed B had the same concentration of *i*-octane as feed A, and feed B had a lower concentration of helium due to the presence of the hydrocarbon. After steady state was obtained, a switching valve directed feed B to the membrane and feed A to the vent, and the transient responses of the *i*-octane and the hydrocarbon were measured with a Pfeiffer Prisma mass spectrometer. A computer allowed detection of multiple mass peaks. *i*-Octane is too large to adsorb in the MFI structure at these conditions so it only flows through defects,[43] and thus the switch to steam B measured the change in the *i*-octane flux through defects due to hydrocarbon adsorption. This system was also used to measure hydrocarbon fluxes by feeding a hydrocarbon/helium stream at steady state. A helium stream with a known concentration of hydrocarbon was fed to the mass spectrometer to calibrate it.

Before each transient experiment, the membrane was heated to 473 K overnight to remove adsorbed species. A stainless steel membrane module used Viton o-rings to seal the membrane, and the feed entered the inside of the tube. The helium sweep carried the permeate flow past a capillary that diverted a small portion of the flow to the mass spectrometer. The mass spectrometer data is presented as a moving average of approximately 2 s. Heating tapes maintained the module at constant temperature. Heating tapes around the syringe pump, feed, permeate, and retentate lines prevented hydrocarbon condensation.

Results and Discussion

Membrane Characterization. As shown in Figure 2, during permporosimetry the helium flow through the membrane at room temperature decreased as the benzene activity increased. At a benzene activity of 1, 65% of the helium flow through the membrane at room temperature was not blocked by benzene. This means that 65% of the helium flow is through defects at room temperature. When *n*-hexane was used for permporosimetry instead of benzene, the results were dramatically different. Only 0.25% of the helium flux was not blocked by *n*-hexane at a loading of 2.7 *n*-hexane molec/u.c. Similar behavior was reported previously.[11,12] Those studies concluded that benzene does not significantly swell MFI crystals, and thus it only blocked helium flow through the MFI structure. However, *n*-hexane decreased the helium flow by almost 3 orders of magnitude. The similar behavior for the membrane in the current study indicates that the defects probably have a similar size, so that crystal expansion when *n*-hexane adsorbed almost sealed the defects.

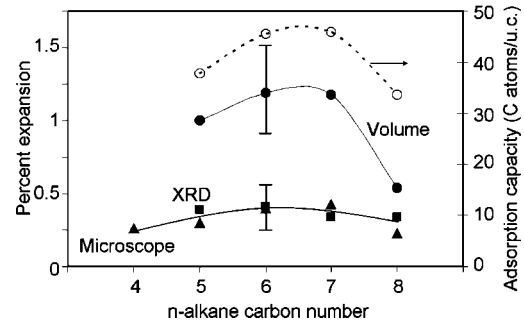

Figure 3. Percent expansion of the *c*-direction of silicalite-1 crystals at 298 K versus the number of carbon atoms in the linear alkane as measured by microscopy (▲) and by XRD (■). The percent volume increase of the unit cell of silicalite-1 from XRD measurements is compared to the adsorption capacity of silicalite-1 (○) from literature data.[48]

Table 2. Change in Silicalite-1/Alkane (At Saturation Loading) Crystal Unit Cell Parameters Measured by XRD as Compared to Unit Cell Dimensions of Silicalite-1 Crystal before Adsorption at Room Temperature

change in unit cell parameter	*n*-pentane	*n*-hexane	*n*-heptane	*n*-octane	*i*-butane	benzene
a (pm)	1.1	5.0	6.2	−0.4	4.2	−1.3
b (pm)	11.2	10.7	10.7	4.3	1.0	0.9
c (pm)	5.3	5.5	4.6	4.6	2.2	0.4
vol (nm^3)	0.0542	0.0644	0.0636	0.0290	0.0226	0.0002
% vol	1.00	1.19	1.18	0.54	0.42	0.00

Table 3. X-ray Diffraction Data for Silicalite-1 Saturated with *n*-Hexane at 180 K

	Morell et al.[28]			current study		
	no adsorbate	*n*-hexane	% change	no adsorbate	*n*-hexane	% change
a (nm)	1.9796	1.9932	0.68	2.0018	2.0035	0.08
b (nm)	2.0037	2.0173	0.67	1.9884	2.0008	0.62
c (nm)	1.3324	1.3419	0.71	1.3323	1.3410	0.65
vol (nm^3)	5.2761	5.3953	2.21	5.3032	5.3756	1.35

The *n*-hexane/DMB ideal selectivity for this membrane was 6 at 300 K for a 50/50 feed at 3.2 kPa. Since the membrane has such a large fraction of its flow through defects, and DMB is only diffusing through defects,[44] the selectivity is not expected to be high. The separation selectivity would be expected to be much higher because the defects would be much smaller in the presence of *n*-hexane, so the DMB flux would be much lower, but the *n*-hexane permeance would be similar.

Optical Microscopy. The size of uncalcined MFI crystals did not change (detection limit = 0.01 μm) when they were exposed to *n*-hexane, *n*-octane, or benzene under the microscope. After template removal by calcination at 723 K, the length of the crystal in the *c*-direction decreased by 0.51% ± 0.17. The error was larger when comparing uncalcined and calcined crystals than for changes due to adsorption because the

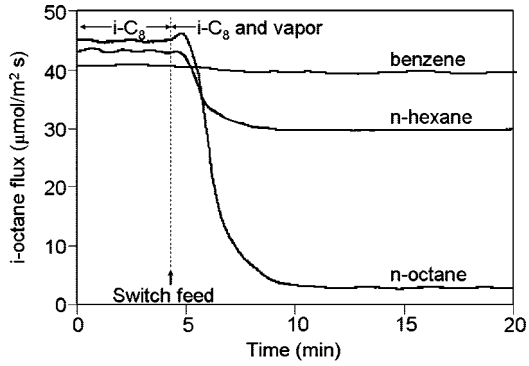

Figure 4. *i*-Octane flux versus time for a MFI membrane at 473 K when benzene (0.12 molec/u.c.), *n*-hexane (1.1 molec/u.c.), and *n*-octane (2.3 molec/u.c.) were added to the feed in separate experiments.

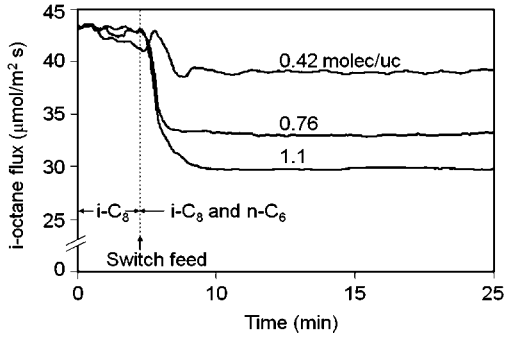

Figure 5. *i*-Octane flux versus time for a MFI membrane at 473 K for three loadings of *n*-hexane added to the feed in separate experiments.

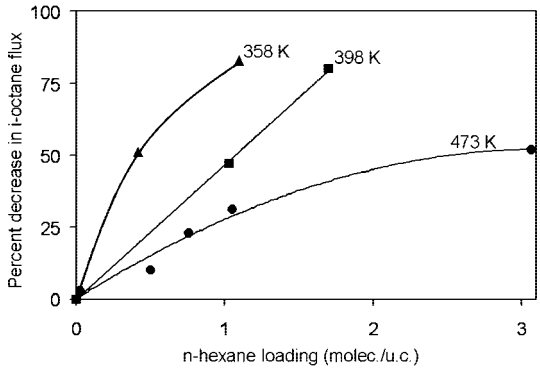

Figure 6. The percent decrease in *i*-octane flux through a MFI membrane as a function of the *n*-hexane loading at three temperatures.

microscope lighting changed when the crystal was removed from the microscope, calcined in the oven, and then returned to the microscope.

Upon exposure to *n*-alkanes, crystal expansion in the *c*-direction was detected by the optical microscope. As shown in Figure 3, the *c*-direction expansion was greatest for *n*-heptane, (0.43%), but the C_4-C_8 *n*-alkanes all caused crystal expansion. Although the microscope only measures expansion in one direction and is less sensitive than XRD, it is a quick screening method for crystal expansion.

X-ray Diffraction. XRD measurements at room temperature showed that after calcination, the MFI crystal shrank 0.47% in the *c*-direction and 0.70% in volume. Bhange et al. reported *c*-direction shrinkage of 0.37% and a volume reduction of 1.0% after template removal from silicalite-1 by heating to 720 K.[45]

Unit cell parameters from room temperature XRD on calcined silicalite-1 were similar to those reported by others for single crystal and powder XRD (Table 1).[37,46,47] The unit cell increased

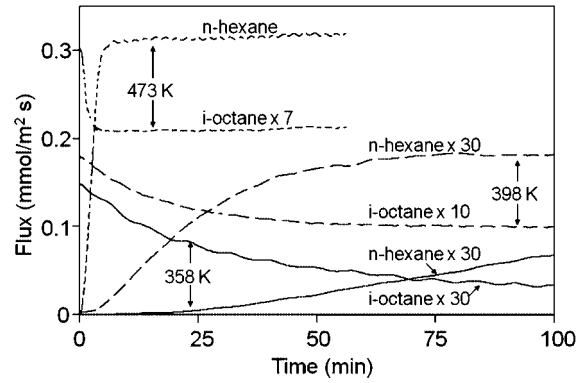

Figure 7. *i*-Octane and *n*-hexane fluxes as a function of time at three temperatures. At time zero, the feed was switched from an *i*-octane/helium mixture to an *i*-octane/*n*-hexane/helium mixture. The fluxes were multiplied by the indicated factors for clarity.

approximately 1.1 vol % following *n*-pentane, *n*-hexane, and *n*-heptane adsorption at room temperature, and the largest expansion was in the *b*-direction for these molecules (Table 2). The unit cell parameters for a crystal before adsorption and the silicalite-1/*n*-hexane crystal are the average of three XRD measurements; the crystal was calcined and then re-exposed to the hydrocarbon for each XRD measurement. Two measurements were made for *n*-octane and benzene, and one for *n*-pentane and *n*-heptane. For C_5-C_8 *n*-alkanes, the *c*-direction expansion was approximately 0.37%. The *b*-direction expansion (~0.54%) was also similar for C_5-C_7 *n*-alkanes, but was only 0.22% for *n*-octane. Figure 3 shows that the percent expansion in the *c*-direction for XRD and microscopy are the same within experimental error. The percent increase in unit cell volume from XRD, also shown in Figure 3, has the same dependence on *n*-alkane carbon number as the adsorption capacity (carbon atoms per unit cell) reported by De Meyer et al.[48] This correlation may be coincidence, and measurements with larger alkanes would be necessary to determine if they are related. As shown in Table 2, *i*-butane increased the unit cell dimension in all three directions, and the volume increased by 0.42%. Thus, both branched and linear alkanes increase the unit cell of MFI crystals. The crystals remained twinned and orthorhombic before and after adsorption.

Unit cell parameters were also measured at 180 K following *n*-hexane adsorption so that a comparison could be made to literature values. The silicalite-1 crystal expanded 1.35 vol % when *n*-hexane adsorbed at 180 K (Table 3), whereas Morell et al. reported a 2.2 vol % expansion for silicalite-1.[30] The crystal before adsorption was 1.0 vol % larger at room temperature than at 180 K, but the silicalite-1/*n*-hexane crystal was only 0.67 vol % larger at room temperature than at 180 K.

Transient Permeation. *i*-Octane transported exclusively through membrane defects because it was too large to adsorb in MFI structure.[43] Thus, the change in *i*-octane flux after adding a second molecule to the feed indicates how the defect size changes following adsorption in the MFI structure. At a coverage of 0.12 molec/u.c., benzene did not significantly change the *i*-octane flux at 473 K, as seen in Figure 4. A *n*-hexane loading of 1.1 molec/u.c. decreased the *i*-octane flux by 25%, and an *n*-octane loading of 2.3 molec/u.c. decreased the *i*-octane flux by 93%. Figure 5 shows that as the *n*-hexane loading increased at 473 K, the percent decrease in *i*-octane flux increased. As seen in Figure 6, the *i*-octane flux decreased as the *n*-hexane loading increased at a given temperature. For the same *n*-hexane loading, the *i*-octane flux decreased more at lower temperature (Figure 6).

The MFI unit cell volume increases from 298 to 570 K,[18] so the defects should be smaller at higher temperature. However, the *i*-octane flux is higher at higher temperature, indicating that the diffusivity increased enough to compensate. The smaller effect of a given *n*-hexane loading at higher temperature (Figure 6) may result because *n*-hexane causes less expansion of the MFI crystal at higher temperature. Although XRD and microscopy measurements were not made above room temperature, the crystals expanded less at room temperature than at 180 K.

The *i*-octane flux reached steady-state within 5 min of adding 1.1 molec/u.c. of *n*-hexane at 473 K (Figure 7). As the temperature decreased at equal loading, the time to steady-state increased from approximately 5 min at 473 K to 80 min at 398 K and then to 260 min at 358 K. The *i*-octane flux decreased in a mirror image of the increase in *n*-hexane flux. The slower adsorption of *n*-hexane at lower temperature seems to decrease the rate of crystal expansion. The *i*-octane flux recovered fully after the flow was switched to pure *i*-octane.

Conclusions

Microscopy and XRD measurements showed that C_4-C_8 *n*-alkane and *i*-butane adsorption at saturation loading increased the size of silicalite-1 crystals at room temperature, and *n*-hexane and *n*-heptane caused the largest increase. A saturation loading of benzene did not significantly change the size of silicalite-1 crystals. Transient permeation measurements showed that crystal expansion by *n*-C_6 and *n*-C_8 adsorption decreased the defect pore size in MFI membranes at 358 to 473 K, even at loadings as low as 0.42−0.50 molec/u.c. The defect sizes decreased less at higher temperatures for the same *n*-alkane loading.

Acknowledgment

We gratefully acknowledge support by the National Science Foundation (NSF) grant CBET 0730047 and a Graduate Assistance in Areas of National Need fellowship to S.G.S. We thank Dr. Mei Hong for preparing the membrane used in these studies and Professor Kristi Anseth for use of the optical microscope. X-ray diffraction was supported in part by NSF grant EAR-0711165.

Literature Cited

(1) Baerlocher, C.; Meier, W. M.; Olson, D. H. *Atlas of Zeolite Framework Types*; 5th ed.; Elsevier: Amsterdam, 2001.

(2) Mohanty, S.; McCormick, A. V. Prospects for principles of size and shape selective separations using zeolites. *Chem. Eng. J.* **1999**, *74*, 1.

(3) Nair, S.; Tsapatsis, M. The location of *o*- and *m*-xylene in silicalite by powder X-ray diffraction. *J. Phys. Chem. B* **2000**, *104*, 8982.

(4) Arruebo, M.; Falconer, J. L.; Noble, R. D. Separation of binary C_5 and C_6 hydrocarbon mixtures through MF1 zeolite membranes. *J. Membr. Sci.* **2006**, *269*, 171.

(5) Coronas, J.; Noble, R. D.; Falconer, J. L. Separations of C_4 and C_6 isomers in ZSM-5 tubular membranes. *Ind. Eng. Chem. Res.* **1998**, *37*, 166.

(6) Flanders, C. L.; Tuan, V. A.; Noble, R. D.; Falconer, J. L. Separation of C_6 isomers by vapor permeation and pervaporation through ZSM-5 membranes. *J. Membr. Sci.* **2000**, *176*, 43.

(7) Gade, S. K.; Tuan, V. A.; Gump, C. J.; Noble, R. D.; Falconer, J. L. Highly selective separation of *n*-hexane from branched, cyclic, and aromatic hydrocarbons using B-ZSM-5 membranes. *Chem. Commun.* **2001**, 601.

(8) Gump, C. J.; Noble, R. D.; Falconer, J. L. Separation of hexane isomers through nonzeolite pores in ZSM-5 zeolite membranes. *Ind. Eng. Chem. Res.* **1999**, *38*, 2775.

(9) Vroon, Z. A. E. P.; Keizer, K.; Gilde, M. J.; Verweij, H.; Burggraaf, A. J. Transport properties of alkanes through ceramic thin zeolite MFI membranes. *J. Membr. Sci.* **1996**, *113*, 293.

(10) Yu, M.; Amundsen, T. J.; Hong, M.; Falconer, J. L.; Noble, R. D. Flexible nanostructure of MFI zeolite membranes. *J. Membr. Sci.* **2007**, *298*, 182.

(11) Lee, J. B.; Funke, H.; Noble, R. D.; Falconer, J. L. High Selectivities in Defective MFI Membranes. *J. Membr. Sci.* **2008**, *323*, 309.

(12) Yu, M.; Falconer, J. L.; Noble, R. D. Characterizing non-zeolitic pore volume in zeolite membranes by temperature-programmed desorption. *Microporous Mesoporous Mater.* **2007**, *106*, 140.

(13) Yu, M.; Falconer, J. L.; Amundsen, T. J.; Hong, M.; Noble, R. D. A controllable nanometer-sized valve. *Adv. Mater.* **2007**, *19*, 3032.

(14) Gatta, G. D.; Nestola, F.; Ballaran, T. B. Elastic behavior, phase transition, and pressure induced structural evolution of analcime. *Am. Mineral.* **2006**, *91*, 568.

(15) Bhange, D. S.; Ramaswamy, V. High temperature thermal expansion behavior of silicalite-1 molecular sieve: in situ HTXRD study. *Microporous Mesoporous Mater.* **2007**, *103*, 235.

(16) Marinkovic, B. A.; Jardim, P. M.; Saavedra, A.; Lau, L. Y.; Baehtz, C.; de Avillez, R. R.; Rizzo, F. Negative thermal expansion in hydrated HZSM-5 orthorhombic zeolite. *Microporous Mesoporous Mater.* **2004**, *71*, 117.

(17) Bhange, D. S.; Ramaswamy, V. Negative thermal expansion in silicalite-1 and zirconium silicalite-1 having MFI structure. *Mater. Res. Bull.* **2006**, *41*, 1392.

(18) Marinkovic, B. A.; Jardim, P. M.; Rizzo, F.; Saavedra, A.; Lau, L. Y.; Suard, E. Complex thermal expansion properties of Al-containing HZSM-5 zeolite: A X-ray diffraction, neutron diffraction and thermogravimetry study. *Microporous Mesoporous Mater.* **2008**, *111*, 110.

(19) Jardim, P. M.; Marinkovic, B. A.; Saavedra, A.; Lau, L. Y.; Baehtz, C.; Rizzo, F. A comparison between thermal expansion properties of hydrated and dehydrated orthorhombic HZSM-5 zeolite. *Microporous Mesoporous Mater.* **2004**, *76*, 23.

(20) Bhange, D. S.; Ramaswamy, V. Thermal stability of the Mobil Five-type metallosilicate molecular sieves—An in situ high, temperature X-ray diffraction study. *Mater. Res. Bull.* **2007**, *42*, 851.

(21) van Koningsveld, H.; Tuinstra, F.; Vanbekkum, H.; Jansen, J. C. The Location of *para*-xylene in a single-crystal of zeolite H-ZSM-5 with a new, sorbate-induced, orthorhombic framework symmetry. *Acta Crystallogr., Sect. B* **1989**, *45*, 423.

(22) Lee, C. K.; Chiang, A. S. T. Adsorption of aromatic compounds in large MFI zeolite crystals. *J. Chem. Soc., Faraday Trans.* **1996**, *92*, 3445.

(23) Bellat, J. P.; Lemaire, E.; Simon, J. M.; Weber, G.; Dubreuil, A. C. Adsorption and coadsorption of 2-methylpentane and 2,2-dimethylbutane in a ZSM-5 zeolite. *Adsorption* **2005**, *11*, 109.

(24) Takaishi, T.; Tsutsumi, K.; Chubachi, K.; Matsumoto, A. Adsorption induced phase transition of ZSM-5 by *p*-xylene. *J. Chem. Soc., Farzday Trans.* **1998**, *94*, 601.

(25) Mentzen, B. F.; Gelin, P. The silicate *p*-xylene system 0.1. flexibility of the MFI framework and sorption mechanism observed during *p*-xylene pore-filling by x-ray-powder diffraction at room-temperature. *Mater. Res. Bull.* **1995**, *30*, 373.

(26) van Koningsveld, H.; Koegler, J. H. Preparation and structure of crystals of zeolite H-ZSM-5 loaded with *p*-nitroaniline. *Microporous Mater.* **1997**, *9*, 71.

(27) Fyfe, C. A.; Kennedy, G. J.; Deschutter, C. T.; Kokotailo, G. T. Sorbate-induced structural-changes in ZSM-5 (silicalite). *J. Chem. Soc., Chem. Commun.* **1984**, 541.

(28) Morell, H.; Angermund, K.; Lewis, A. R.; Brouwer, D. H.; Fyfe, C. A.; Gies, H. Structural investigation of silicalite-I loaded with *n*-hexane by X-ray diffraction, Si-29 MAS NMR, and molecular modeling. *Chem. Mater.* **2002**, *14*, 2192.

(29) Mentzen, B. F.; Lefebvre, F. Flexibility of the MFI silicalite framework upon benzene adsorption at higher pore-fillings: A study by X-ray powder diffraction, NMR and molecular mechanics. *Mater. Res. Bull.* **1997**, *32*, 813.

(30) Morell, H. Analyse der Gast-Wirt-Wechselwirkungen von *n*-alkanen C_6-C_{12} im kanalsystem von silicalit-I. Thesis. Ruhr-Universitat Bochum, Bochum, Germany, 2001.

(31) Mohanty, S.; Davis, H. T.; McCormick, A. V. Sorbate/sorbent phase transition during adsorption of *p*-xylene in silicalite. *AlChE J.* **2000**, *46*, 1662.

(32) Tuel, A.; Caldarelli, S.; Meden, A.; McCusker, L. B.; Baerlocher, C.; Ristic, A.; Rajic, N.; Mali, G.; Kaucic, V. NMR characterization and Rietveld refinement of the structure of rehydrated AlPO4−34. *J. Phys. Chem. B* **2000**, *104*, 5697.

(33) Boulicaut, L.; Brandani, S.; Ruthven, D. M. Liquid phase sorption and diffusion of branched and cyclic hydrocarbons in silicalite. *Microporous Mesoporous Mater.* **1998**, *25*, 81.

(34) Kornatowski, J. Growth of large crystals of ZSM-5 zeolite. *Zeolites* **1988**, *8*, 77.

(35) Kocirik, M.; Kornatowski, J.; Masarik, V.; Novak, P.; Zikanova, A.; Maixner, J. Investigation of sorption and transport of sorbate molecules

in crystals of MFI structure type by iodine indicator technique. *Microporous Mesoporous Mater.* **1998**, *23*, 295.

(36) Brabec, L.; Kocirik, M. Silicalite-1 polycrystalline layers and crystal twins: Morphology and grain boundaries. *Mater. Chem. Phys.* **2007**, *102*, 67.

(37) Rieder, M.; Klementova, M.; Brabec, L.; Kocirik, M. Morphology and structure of silicalite-1 crystals. Evidence of twinning by X-ray and electron diffraction. *Stud. Surf. Sci. Catal.* **2005**, *158*, 741.

(38) Tuan, V. A.; Noble, R. D.; Falconer, J. L. Boron-substituted ZSM-5 membranes: Preparation and separation performance. *AlChE J.* **2000**, *46*, 1201.

(39) Bakker, W. J. W.; Kapteijn, F.; Poppe, J.; Moulijn, J. A. Permeation characteristics of a metal-supported silicalite-1 zeolite membrane. *J. Membr. Sci.* **1996**, *117*, 57.

(40) Chen, Z. X.; Lu, J. G.; Liu, X. Y.; Ding, T. F. Adsorption equilibria of *n*-alkanes on silicalite and ZSM-5. *Chin. J. Chem. Eng.* **2000**, *8*, 283.

(41) Krishna, R.; Paschek, D. Separation of hydrocarbon mixtures using zeolite membranes: a modelling approach combining molecular simulations with the Maxwell−Stefan theory. *Sep. Purif. Technol.* **2000**, *21*, 111.

(42) Wu, P. D.; Debebe, A.; Yi, H. M. Adsorption and Diffusion of C_6 and C_8 Hydrocarbons in Silicalite. *Zeolites* **1983**, *3*, 118.

(43) Chen, N. Y.; Garwood, W. E. Some Catalytic Properties of ZSM-5, a New Shape Selective Zeolite. *J. Catal.* **1978**, *52*, 453.

(44) Yu, M.; Wyss, J. C.; Noble, R. D.; Falconer, J. L. 2,2-Dimethylbutane adsorption and diffusion in MFI zeolite. *Microporous Mesoporous Mater.* **2008**, *111*, 24.

(45) Bhange, D. S.; Pandya, N. A.; Jha, R. K.; Ramaswamy, V. Non-isothermal kinetic studies of the template decomposition from silicalite-1 framework—high temperature X-ray diffraction and thermogravimetric analysis. *Microporous Mesoporous Mater.* **2007**, *113*, 64.

(46) Olson, D. H.; Kokotailo, G. T.; Lawton, S. L.; Meier, W. M. Crystal-Structure and structure-related properties of ZSM-5. *J. Phys. Chem.* **1981**, *85*, 2238.

(47) Price, G. D.; Pluth, J. J.; Smith, J. V.; Bennett, J. M.; Patton, R. L. Crystal-structure of tetrapropylammonium fluoride containing precursor to fluoride silicalite. *J. Am. Chem. Soc.* **1982**, *104*, 5971.

(48) De Meyer, K. M. A.; Chempath, S.; Denayer, J. F. M.; Martens, J. A.; Snurr, R. Q.; Baron, G. V. Packing effects in the liquid-phase adsorption of C_5−C_{22} *n*-alkanes on ZSM-5. *J. Phys. Chem. B* **2003**, *107*, 10760.

Received for review April 18, 2008
Revised manuscript received September 24, 2008
Accepted September 29, 2008

IE800630G